

# Spontaneous parity and charge-conjugation violations at real isospin and imaginary baryon chemical potentials

Hiroaki Kouno,<sup>1,\*</sup> Mizuho Kishikawa,<sup>2</sup> Takahiro Sasaki,<sup>3,†</sup> Yuji Sakai,<sup>3,‡</sup> and Masanobu Yahiro<sup>3,§</sup>

<sup>1</sup>*Department of Physics, Saga University, Saga 840-8502, Japan*

<sup>2</sup>*E.I.M. Electric Corporation Limited, Fukuoka 807-0001, Japan*

<sup>3</sup>*Department of Physics, Graduate School of Sciences, Kyushu University, Fukuoka 812-8581, Japan*

(Dated: February 18, 2022)

The phase structure of two-flavor QCD is investigated at real isospin and imaginary quark chemical potentials by using the Polyakov-loop extended Nambu–Jona-Lasinio model. In the region, parity symmetry is spontaneously broken by the pion superfluidity phase transition, whereas charge-conjugation symmetry is spontaneously violated by the Roberge-Weiss transition. The chiral (deconfinement) crossover at zero isospin and quark chemical potentials is a remnant of the parity (charge-conjugation) violation. The interplay between the parity and charge-conjugation violations are analyzed, and it is investigated how the interplay is related to the correlation between the chiral and deconfinement crossovers at zero isospin and quark chemical potentials.

PACS numbers: 11.30.Rd, 12.40.-y

## I. INTRODUCTION

The phase diagram of Quantum Chromodynamics (QCD) is the key to understanding not only natural phenomena such as compact stars and the early universe but also laboratory experiments such as relativistic heavy-ion collisions. Quantitative calculations of the phase diagram with the first-principle lattice QCD (LQCD) have the well-known sign problem when the baryon chemical potential  $\mu_B$  is real [1]; here  $\mu_B = 3\mu_q$  for the quark-number chemical potential  $\mu_q$ .

The grand canonical partition function  $Z(\mu_q)$  of two-flavor QCD can be obtained by

$$Z(\mu_q) = \int \mathcal{D}U \det \Delta(\mu_q) e^{-S_G}, \quad (1)$$

where  $\int \mathcal{D}U$  denotes the path integral with respect to gauge variable  $U$ ,  $S_G$  stands for the pure gauge action and

$$\Delta(\mu_q) = D_\nu \gamma_\nu + m_0 - \mu_q \gamma_4 \quad (2)$$

with the gamma matrix  $\gamma_\mu$  in the Euclidean notation and the quark mass  $m_0$ . For simplicity, up and down quarks are assumed to have the same mass  $m_0$ . When  $\mu_q$  is real, it is easy to verify

$$\Delta(\mu_q)^\dagger = -D_\nu \gamma_\nu + m_0 - \mu_q \gamma_4 = \gamma_5 \Delta(-\mu_q) \gamma_5. \quad (3)$$

This leads to

$$\begin{aligned} \{\det \Delta(\mu_q)\}^* &= \det \{\gamma_5 \Delta(-\mu_q) \gamma_5\} \\ &= \det \Delta(-\mu_q) \neq \det \Delta(\mu_q), \end{aligned} \quad (4)$$

and hence  $\det \Delta(\mu_q)$  is complex. This causes the sign problem. Several approaches have been proposed so far to circumvent the difficulty; for example, the reweighting method [2],

the Taylor expansion method [3] and the analytic continuation from imaginary  $\mu_q$  to real  $\mu_q$  [4–12]. However, those are still far from perfection particularly at  $\mu_q/T \gtrsim 1$ , where  $T$  is temperature.

As an approach complementary to LQCD, we can consider effective models such as the Nambu–Jona-Lasinio (NJL) model [13–28] and the Polyakov-loop extended Nambu–Jona-Lasinio (PNJL) model [29–72]. The NJL model describes the chiral symmetry breaking, but not the confinement mechanism. The PNJL model is extended so as to treat both the mechanisms approximately by considering the Polyakov loop in addition to the chiral condensate as ingredients of the model.

In the NJL-type models, the input parameters are usually determined from the pion mass and the pion decay constant at vacuum ( $\mu_q = 0$  and  $T = 0$ ). It is then highly nontrivial whether the models properly predict the dynamics of QCD at finite  $\mu_q$ . This should be tested from QCD. Such a test is possible at imaginary  $\mu_q$  and finite isospin chemical potential, since LQCD has no sign problem there.

For imaginary quark chemical potential,  $\mu_q = i\theta T$ , one can verify that

$$\Delta(i\theta T)^\dagger = -D_\nu \gamma_\nu + m_0 + i\theta T \gamma_4 = \gamma_5 \Delta(i\theta T) \gamma_5. \quad (5)$$

This leads to

$$\{\det \Delta(i\theta T)\}^* = \det \{\gamma_5 \Delta(i\theta T) \gamma_5\} = \det \Delta(i\theta T), \quad (6)$$

and hence  $\det \Delta(i\theta T)$  is real. LQCD has thus no sign problem at imaginary  $\mu_q$ .

At imaginary  $\mu_q$ , the QCD partition function has the Roberge-Weiss (RW) periodicity, i.e. the periodicity of  $2\pi/3$  in  $\theta$ . The RW periodicity is a remnant of the  $\mathbb{Z}_3$  symmetry in the pure gauge limit. This periodicity can be reinterpreted as the extended  $\mathbb{Z}_3$  symmetry [47, 48, 52, 54]; see (30)–(33) for the relation between the RW periodicity and the extended  $\mathbb{Z}_3$  symmetry. At higher  $T$ , three  $\mathbb{Z}_3$  vacua emerge one by one [73] as  $\theta$  increases. This mechanism guarantees the extended  $\mathbb{Z}_3$  symmetry (the RW periodicity) at higher  $T$ . The mechanism induces the first-order phase transition at

\*kounoh@cc.saga-u.ac.jp

†sasaki@phys.kyushu-u.ac.jp

‡sakai@phys.kyushu-u.ac.jp

§yahiro@phys.kyushu-u.ac.jp

$\Theta = (2k+1)\pi/3$ , where  $k$  is an integer [73]. This phase transition is called the RW transition. The partition function of the PNJL model has the extended  $\mathbb{Z}_3$  symmetry and hence yields the RW periodicity and the RW transition [48, 55, 70–72]. Eventually, the PNJL model qualitatively reproduces LQCD data [48].

LQCD simulations at imaginary  $\mu_q$  show that the chiral and deconfinement crossovers take place simultaneously [4–12]. Such a strong correlation between the transitions is not seen in the original PNJL model [48, 52, 57]. We then extended the PNJL model to solve this problem. In the new model called the entanglement PNJL (EPNJL) model, the strength of the four-quark vertex depends on the Polykov loop [63]. In the EPNJL model, the chiral and deconfinement crossovers coincide with each other, so that the EPNJL model yields good agreement with LQCD data [63].

The reliability of the PNJL and EPNJL models can be tested at finite isospin chemical potential ( $\mu_{\text{iso}}$ ), since LQCD has no sign problem there [74]. For later convenience, we use the “modified” isospin chemical potential  $\mu_I = \mu_{\text{iso}}/2$  instead of  $\mu_{\text{iso}} = \mu_u - \mu_d$ , where  $\mu_u$  and  $\mu_d$  are chemical potentials for up and down quarks, respectively. The QCD partition function at finite  $\mu_I$  is obtained by

$$\begin{aligned} Z(\mu_I) &= \int \mathcal{D}U \det \Delta(\mu_u) \det \Delta(\mu_d) e^{-S_G} \\ &= \int \mathcal{D}U \det \Delta(\mu_I) \det \Delta(-\mu_I) e^{-S_G}. \end{aligned} \quad (7)$$

When  $\mu_u$  and  $\mu_d$  are pure imaginary, both  $\det \Delta(\mu_q)$  and  $\det \Delta(\mu_q)$  are real as shown in (6). When  $\mu_u$  and  $\mu_d$  are real, it is possible to prove that

$$\{\det \Delta(\mu_I) \det \Delta(-\mu_I)\}^* = \det \Delta(\mu_I) \det \Delta(-\mu_I). \quad (8)$$

The product of the two determinants is thus real, whereas each of the determinants is not. LQCD has hence no sign problem for both real and imaginary  $\mu_I$ . Actually, LQCD data are available there; see Refs. [8, 75] for real  $\mu_I$  and Refs. [7, 8] for imaginary  $\mu_I$ .

The PNJL model explains the LQCD data qualitatively not only at real  $\mu_I$  [36, 37, 62] and but also at imaginary  $\mu_I$  [57]; the eight-quark interaction newly added improves the agreement between the PNJL result and the LQCD data [62]. The EPNJL model reproduces the LQCD data quantitatively with no free parameter; note that all the parameters in the EPNJL model are fixed at vacuum and at imaginary chemical potential. As for real  $\mu_I$ , there exists a tricritical point (TCP), i.e. a meeting point between the first- and second-order pion-superfluidity phase-transition lines. The location of the TCP is predicted by the EPNJL model [63] as well as the PNJL model [36, 62], the chiral perturbation theory [74], the strong coupling QCD [76] and so on [77].

As for real  $\mu_q$ , LQCD data are available at small  $\mu_q/T$  with the Taylor expansion method [3]. The EPNJL model reproduces the LQCD data quantitatively with no free parameter [67]. The EPNJL model predicts [63] that there is a critical endpoint (CEP) [14, 78] of the first-order chiral transition in the  $\mu_q$ - $T$  plane.

LQCD has no sign problem also at real isospin and imagi-

nary quark chemical potentials, because

$$\begin{aligned} &\{\det \Delta(\mu_I + i\Theta T) \det \Delta(-\mu_I + i\Theta T)\}^* \\ &= \det \Delta(\mu_I + i\Theta T) \det \Delta(-\mu_I + i\Theta T) \end{aligned} \quad (9)$$

for  $\mu_u = \mu_I + i\Theta T$  and  $\mu_d = -\mu_I + i\Theta T$ . The reliability of the PNJL and EPNJL models can be checked also in this case, although no LQCD data is available at the present stage. It should be noted that the LQCD calculation with real  $\mu_I$  and imaginary  $\mu_q$  is equivalent to the LQCD calculation with complex quark number chemical potential under the phase quenched approximation [79].

There is a debate whether the chiral and deconfinement transitions at  $\mu_q = \mu_I = 0$  coincide or not; see Ref. [80] and references therein. If the two transitions do not coincide, exotic phases such as the constituent-quark phase [81, 82] or the quarkyonic phase [46, 51, 53, 83, 84] may appear. However, the chiral and deconfinement transitions are confirmed to be crossover with LQCD [85, 86], so that transition temperatures of the two crossovers are not well defined. The coincidence problem thus includes conceptual difficulty.

As a way of circumventing the conceptual difficulty in the coincidence problem, we should consider exact phase transitions relevant to the chiral and deconfinement crossovers. This is really possible. It is reported with the EPNJL model [66] that the chiral and deconfinement transitions coincide when the parity ( $P$ ) restoration and the charge-conjugation ( $C$ ) violation occur simultaneously at  $\theta = \Theta = \pi$ , where  $\theta$  is the parameter of the  $\theta$ -vacuum [25–28]. The chiral and deconfinement crossovers at  $\mu_q = \mu_I = 0$  are remnants of the  $P$  restoration and the  $C$  violation at  $\theta = \Theta = \pi$ , respectively. LQCD has, however, the sign problem at finite  $\theta$  and hence it is difficult to check the validity of the model prediction with LQCD. Such a problem does not appear at  $\mu_I > 0$  and  $\Theta = \pi$ , as mentioned above.

In this paper, we investigate the interplay between the pion-superfluidity and RW phase transitions in the region of  $\Theta = \pi$  and  $\mu_I > m_\pi/2$ , using the PNJL and EPNJL models; here  $m_\pi$  is the pion mass in the vacuum. In the region, the  $P$  violation due to the pion-superfluidity transition occurs at lower  $T$ , whereas the  $C$  violation due to the RW transition takes place at higher  $T$ . These transitions are exact phase transitions and hence we can define the order parameters without any ambiguity. We also investigate the relation between the chiral transition at  $\mu_I = \Theta = 0$  and the  $P$  violation at  $\Theta = 0$  and  $\mu_I > m_\pi/2$  by varying  $\mu_I$  and the relation between the deconfinement transition at  $\mu_I = \Theta = 0$  and the  $C$  violation at  $\Theta = \pi$  and  $\mu_I = 0$  by varying  $\Theta$ . Finally we discuss how the correlation between the  $P$  and  $C$  violations at  $\Theta = \pi$  and  $\mu_I > m_\pi/2$  is related to the correlation between the chiral and deconfinement crossovers at  $\mu_I = \Theta = 0$ . In future, we can check the model prediction made in this paper by using LQCD, since LQCD has no sign problem in the region and hence LQCD simulations are feasible.

This paper is organized as follows. In section II, we explain the PNJL and EPNJL models. In section III, numerical results are shown. Section IV is devoted to summary.

## II. PNJL MODEL

The two-flavor PNJL Lagrangian in Euclidean space-time is

$$\mathcal{L} = \bar{q}(\gamma_\nu D_\nu - \tilde{\mu}\gamma_4 + \tilde{m}_0)q - G_s [(\bar{q}q)^2 + (\bar{q}i\gamma_5\vec{\tau}q)^2] + \mathcal{U}(\Phi[A], \Phi[A]^*, T), \quad (10)$$

where  $D_\nu = \partial_\nu - iA_\nu$  and  $A_\nu = \delta_{\nu,4}gA_{4,a}\frac{\lambda_a}{2}$  with the gauge field  $A_{\nu,a}$ , the Gell-Mann matrix  $\lambda_a$  and the gauge coupling  $g$ . In the NJL sector  $G_s$  denotes the coupling constant of the scalar-type four-quark interaction. As is seen later, the Polyakov potential  $\mathcal{U}$  is a function of the Polyakov loop  $\Phi$  and its Hermitian conjugate  $\Phi^*$ .

The quark mass matrix  $\tilde{m}_0$  is given by  $\tilde{m}_0 = \text{diag}(m_0, m_0)$ . The chemical potential matrix  $\tilde{\mu}$  is defined by  $\tilde{\mu} = \text{diag}(\mu_u, \mu_d)$  with the  $u$ -quark ( $d$ -quark) number chemical potential  $\mu_u$  ( $\mu_d$ ). This is equivalent to introducing the baryon and isospin chemical potentials,  $\mu_B$  and  $\mu_{\text{iso}}$ , coupled respectively to the baryon charge  $\hat{B}$  and to the isospin charge  $\hat{I}_3$ :

$$\tilde{\mu} = \mu_q\tau_0 + \mu_I\tau_3 \quad (11)$$

with

$$\mu_q = \frac{\mu_u + \mu_d}{2} = \frac{\mu_B}{3}, \quad \mu_I = \frac{\mu_u - \mu_d}{2} = \frac{\mu_{\text{iso}}}{2}, \quad (12)$$

where  $\tau_0$  is the unit matrix and  $\tau_i$  ( $i = 1, 2, 3$ ) are the Pauli matrices in the flavor space. Note that  $\mu_q$  is the quark chemical potential and  $\mu_I$  is half the isospin chemical potential ( $\mu_{\text{iso}}$ ). In the limit of  $m_0 = \mu_I = 0$ , the PNJL Lagrangian has the  $SU_L(2) \times SU_R(2) \times U_v(1) \times SU_c(3)$  symmetry. For  $m_0 \neq 0$  and  $\mu_I \neq 0$ , it is reduced to  $U_{I_3}(1) \times U_v(1) \times SU_c(3)$ .

The Polyakov loop operator  $\hat{\Phi}$  and its Hermitian conjugate  $\hat{\Phi}^\dagger$  are defined as

$$\hat{\Phi} = \frac{1}{N}\text{Tr}L, \quad \hat{\Phi}^\dagger = \frac{1}{N}\text{Tr}L^\dagger, \quad (13)$$

with

$$L(\mathbf{x}) = \mathcal{P} \exp \left[ i \int_0^\beta d\tau A_4(\mathbf{x}, \tau) \right], \quad (14)$$

where  $\mathcal{P}$  is the path ordering and  $A_4 = iA_0$ . In the PNJL model, the vacuum expectation values,  $\Phi = \langle \hat{\Phi} \rangle$  and  $\Phi^* = \langle \hat{\Phi}^\dagger \rangle$ , are treated as classical variables. In the Polyakov gauge,  $L$  can be written in a diagonal form in color space [31]:

$$L = e^{i\beta(\phi_3\lambda_3 + \phi_8\lambda_8)} = \text{diag}(e^{i\beta\phi_a}, e^{i\beta\phi_b}, e^{i\beta\phi_c}), \quad (15)$$

where  $\phi_a = \phi_3 + \phi_8/\sqrt{3}$ ,  $\phi_b = -\phi_3 + \phi_8/\sqrt{3}$  and  $\phi_c = -(\phi_a + \phi_b) = -2\phi_8/\sqrt{3}$ .

The Polyakov loop  $\Phi$  is an exact order parameter of the spontaneous  $\mathbb{Z}_3$  symmetry breaking in the pure gauge theory. Although the  $\mathbb{Z}_3$  symmetry is not exact in the system with dynamical quarks, it still seems to be a good indicator of the

deconfinement phase transition. Therefore, we use  $\Phi$  to define the deconfinement phase transition.

The spontaneous breakings of the chiral and the  $U_{I_3}(1)$  symmetry are described by the chiral condensate  $\sigma = \langle \bar{q}q \rangle$  and the charged pion condensate [21, 22, 36, 62]

$$\pi^\pm = \frac{\pi}{\sqrt{2}} e^{\pm i\varphi} = \langle \bar{q}i\gamma_5\tau_\pm q \rangle, \quad (16)$$

where  $\tau_\pm = (\tau_1 \pm i\tau_2)/\sqrt{2}$ . Since the phase  $\varphi$  represents the direction of the  $U_{I_3}(1)$  symmetry breaking, we take  $\varphi = 0$  for convenience. The pion condensate is then expressed by

$$\pi = \langle \bar{q}i\gamma_5\tau_1 q \rangle. \quad (17)$$

Making the mean field (MF) approximation [36, 45, 62], one can obtain the MF Lagrangian as

$$\mathcal{L}_{\text{MF}} = \bar{q}(\gamma_\nu D_\nu - \tilde{\mu}\gamma_4 + M\tau_0 + N i\gamma_5\tau_1)q + G_s[\sigma^2 + \pi^2] + \mathcal{U} \quad (18)$$

with

$$M = m_0 - 2G_s\sigma, \quad (19)$$

$$N = -2G_s\pi. \quad (20)$$

Performing the path integral in the PNJL partition function

$$Z_{\text{PNJL}} = \int Dq D\bar{q} \exp \left[ - \int d^4x \mathcal{L}_{\text{MF}} \right], \quad (21)$$

we can get the thermodynamic potential  $\Omega$  (per unit volume),

$$\begin{aligned} \Omega = -T \ln(Z_{\text{PNJL}})/V = -2 \sum_{i=\pm} \int \frac{d^3p}{(2\pi)^3} & \left[ 3E_i(p) \right. \\ & + \frac{1}{\beta} \ln [1 + 3(\Phi + \Phi^* e^{-\beta E_i^-(p)}) e^{-\beta E_i^-(p)} + e^{-3\beta E_i^-(p)}] \\ & + \frac{1}{\beta} \ln [1 + 3(\Phi^* + \Phi e^{-\beta E_i^+(p)}) e^{-\beta E_i^+(p)} + e^{-3\beta E_i^+(p)}] \\ & \left. + G_s[\sigma^2 + \pi^2] + \mathcal{U} \right] \end{aligned} \quad (22)$$

with  $E_\pm^\pm(p) = E_\pm(p) \pm \mu_q$ , where

$$E_\pm(p) = \sqrt{(E(p) \pm \mu_I)^2 + N^2} \quad (23)$$

for  $E(p) = \sqrt{\mathbf{p}^2 + M^2}$ . On the right-hand side of (22), only the first term diverges, and it is then regularized by the three-dimensional momentum cutoff  $\Lambda$  [31, 34].

We use  $\mathcal{U}$  of Ref. [35] that is fitted to LQCD data in the pure gauge theory at finite  $T$  [87, 88]:

$$\begin{aligned} \mathcal{U} = T^4 \left[ -\frac{a(T)}{2} \Phi^* \Phi \right. \\ \left. + b(T) \ln(1 - 6\Phi\Phi^* + 4(\Phi^3 + \Phi^{*3}) - 3(\Phi\Phi^*)^2) \right], \end{aligned} \quad (24)$$

$$a(T) = a_0 + a_1 \left( \frac{T_0}{T} \right) + a_2 \left( \frac{T_0}{T} \right)^2, \quad b(T) = b_3 \left( \frac{T_0}{T} \right)^3, \quad (25)$$

where parameters are summarized in Table I. The Polyakov potential yields a first-order deconfinement phase transition at  $T = T_0$  in the pure gauge theory. The original value of  $T_0$  is 270 MeV determined from the pure gauge LQCD data, but the PNJL model with this value of  $T_0$  yields a larger value of the pseudocritical temperature  $T_c$  at zero chemical potential than  $T_c = 173 \pm 8$  MeV predicted by the full LQCD simulation [85, 89, 90]. We then reset  $T_0$  to 212 MeV [52] so as to reproduce the LQCD result.

$a_0$	$a_1$	$a_2$	$b_3$
3.51	-2.47	15.2	-1.75

TABLE I: Summary of the parameter set in the Polyakov-potential sector determined in Ref. [35]. All parameters are dimensionless.

Table II shows parameters in the NJL sector used in the present analyses. This set can reproduce the pion decay constant  $f_\pi = 93.3$  MeV and the pion mass  $m_\pi = 138$  MeV at vacuum ( $T = \mu_q = \mu_l = 0$ ).

$G_s$	$m_0$	$\Lambda$
5.498 [GeV <sup>-2</sup> ]	5.5 [MeV]	631.5 [MeV]

TABLE II: Summary of parameters in the NJL sector.

The classical variables  $X = \Phi, \Phi^*, \sigma$  and  $\pi$  are determined by the stationary conditions

$$\partial\Omega/\partial X = 0. \quad (26)$$

The solutions to the stationary conditions do not give the global minimum of  $\Omega$  necessarily. There is a possibility that they yield a local minimum or even a maximum. We then have checked that the solutions yield the global minimum when the solutions  $X(T, \mu_q, \mu_l)$  are inserted into (22).

The thermodynamic potential (22) is invariant under the parity transformation

$$\pi \rightarrow -\pi. \quad (27)$$

Parity odd quantity such as the pion condensate is an order parameter of  $P$  symmetry. When pion condensates,  $P$  symmetry is spontaneously broken [74].

When  $\mu_l \neq 0$ , charge-conjugation symmetry is explicitly broken even at  $\mu_q = 0$  [55, 66], since  $u$  and  $d$  quarks have different electric charge. In the present system where the electromagnetic field is switched off, however, we can neglect the electric charges and consider only a charge-conjugation transformation associated with baryon and color charges. We refer to symmetry under the transformation as partial charge-conjugation symmetry ( $\tilde{C}$ ) in this paper. As far as  $\Omega$  of (22) is concerned, the transformation is simply represented by

$$\phi \rightarrow -\phi \quad (28)$$

with  $\phi$  the phase of the Polyakov loop  $\Phi$ . When  $\mu_q = i\theta T = in\pi T$  for any integer  $n$ ,  $\Omega$  is  $\tilde{C}$ -invariant. As shown below,  $\tilde{C}$

symmetry is spontaneously broken at higher temperature for odd  $n$ .

The thermodynamic potential  $\Omega$  of (22) has a trivial periodicity of  $2\pi$  in  $\theta$ . We then mainly consider one circle,  $0 \leq \theta \leq 2\pi$ . In addition,  $\Omega$  has the RW periodicity [73]. The thermodynamical potential  $\Omega$  is not invariant under the  $\mathbb{Z}_3$  transformation,

$$\Phi \rightarrow \Phi e^{-i2\pi k/3}, \quad \Phi^* \rightarrow \Phi^* e^{i2\pi k/3}, \quad (29)$$

for any integer  $k$ , while  $\mathcal{U}$  of (24) is invariant. Instead of the  $\mathbb{Z}_3$  symmetry, however,  $\Omega$  is invariant under the extended  $\mathbb{Z}_3$  transformation [48],

$$e^{\pm i\theta} \rightarrow e^{\pm i(\theta + \frac{2\pi k}{3})}, \quad \Phi \rightarrow \Phi e^{-i\frac{2\pi k}{3}}, \quad \Phi^* \rightarrow \Phi^* e^{i\frac{2\pi k}{3}}. \quad (30)$$

The extended  $\mathbb{Z}_3$  symmetry guarantees the RW periodicity, as shown below. The thermodynamic potential (22) can be rewritten with the modified Polyakov loop

$$\Psi = \Phi e^{i\theta} \quad (31)$$

invariant under the extended- $\mathbb{Z}_3$  transformation:

$$\begin{aligned} \Omega = -T \ln(Z_{\text{PNJL}})/V = & -2 \sum_{i=\pm} \int \frac{d^3p}{(2\pi)^3} \left[ 3E_i(p) \right. \\ & + \frac{1}{\beta} \ln [1 + 3\Psi e^{-\beta E_i(p)} \\ & + 3\Psi^* e^{-2\beta E_i(p)} e^{i3\theta} + e^{-3\beta E_i(p)} e^{3i\theta}] \\ & + \frac{1}{\beta} \ln [1 + 3\Psi^* e^{-\beta E_i(p)} \\ & + 3\Psi e^{-2\beta E_i(p)} e^{-i3\theta} + e^{-3\beta E_i(p)} e^{-3i\theta}] + G_s[\sigma^2 + \pi^2] \\ & + T^4 \left[ -\frac{a(T)}{2} \Psi^* \Psi \right. \\ & \left. \left. + b(T) \ln(1 - 6\Psi\Psi^* + 4(\Psi^3 e^{-3i\theta} + \Psi^{*3} e^{3i\theta}) - 3(\Psi\Psi^*)^2) \right] \right]. \end{aligned} \quad (32)$$

Obviously,  $\Omega$  is extended- $\mathbb{Z}_3$  invariant, since it depends on  $\theta$  only through the factor  $e^{3i\theta}$ . The factor also guarantees that

$$\Omega(T, \theta) = \Omega(T, \theta + \frac{2\pi}{3}) = \Omega(T, \theta + \frac{4\pi}{3}). \quad (33)$$

Thus,  $\Omega(\theta)$  has a shorter period  $2\pi/3$  in  $\theta$ . This periodicity was first found by Roberge and Weiss [73] for QCD and now it is called the Roberge-Weiss (RW) periodicity. Using the perturbation theory and the strong-coupling lattice theory, Roberge and Weiss also found that a first-order phase transition occurs at  $\theta = \pi/3 \bmod 2\pi/3$  when  $T$  is higher than some critical value  $T_C$ . The transition is also called the Roberge-Weiss transition. After the theoretical prediction, the RW periodicity and the RW transition were confirmed by LQCD [4–12]. Recently, the RW periodicity and the RW transition were also confirmed by Holographic QCD [91]. The RW transition induces the  $C$  breaking [55, 66] for  $\mu_l = 0$  and the  $\tilde{C}$  breaking for  $\mu_l \neq 0$ . The  $C$  and  $\tilde{C}$  breakings occur at  $\theta = \pi$

and the  $\mathbb{Z}_3$  images of the breakings also appear at  $\Theta = i\pi/3$  and  $i5\pi/3$ . It is convenient to use the phase  $\psi$  of the modified Polyakov loop  $\tilde{\Psi}$  as an order parameter of the  $C$  and  $\tilde{C}$  breakings [55, 66]. When  $C$  or  $\tilde{C}$  symmetry is preserved,  $\psi$  vanishes; here we consider  $\psi$  in the region  $-\pi \leq \psi \leq \pi$ .

In LQCD simulations at imaginary  $\mu_q$ , the chiral and deconfinement transitions take place simultaneously, although they are crossover [4–12]. Such a strong correlation can not be reproduced by the PNJL model [48, 52, 57]. This problem is solved by the entanglement PNJL (EPNJL) model [63]. In the EPNJL model, the four-quark vertex depends on the Polyakov loop. In QCD, the four-quark vertex is generated by the gluon propagation between two quarks. If the gluon has a finite vacuum expectation value in its time component, the gluon propagation can depend on  $\Phi$  through the vacuum expectation value [63]. In fact, recent calculations [92–94] of the exact renormalization group equation (ERGE) [95] suggest that mixing interactions between  $\sigma$  and  $\Phi$  are induced. It is highly expected that the functional form and the strength of the entanglement vertex are determined in future by ERGE. In Ref. [63], the following  $\Phi$  dependence of  $G$  is assumed by respecting the chiral symmetry,  $P$  symmetry,  $C$  symmetry and the extended  $\mathbb{Z}_3$  symmetry:

$$G(\Phi) = G[1 - \alpha_1 \Phi \Phi^* - \alpha_2 (\Phi^3 + \Phi^{*3})]. \quad (34)$$

In the EPNJL model, the chiral and deconfinement crossovers coincide at zero chemical potential. The EPNJL model with the parameter set,  $\alpha_1 = \alpha_2 = 0.2$  and  $T_0 = 190$  MeV, can reproduce LQCD data at imaginary chemical potential [63], real isospin chemical potential [63] and small  $\mu_q/T$  [67]. The agreement between LQCD data and the EPNJL result persists also under strong magnetic field [65, 96]. We then use the EPNJL model with this parameter set also in this paper.

The entanglement vertex  $G(\Phi)$  agrees with the parameter  $G$  at  $T = 0$  since  $\Phi = 0$  there. At vacuum the EPNJL model is then reduced to the NJL model; note that the PNJL model agrees with the NJL model at vacuum. As a merit of this property, the NJL sector of the EPNJL model has the same values of parameters as the NJL model.

Very recently, it was shown that the coincidence problem between the chiral and deconfinement transitions does not occur also in the nonlocal PNJL model [71]. In the model, the entanglement between  $\sigma$  and  $\Phi$  naturally appears in the renormalization factor. It is then interesting as a future work to study the relation between the nonlocal PNJL and the EPNJL model.

### III. NUMERICAL RESULTS

#### A. Results at $\mu_l = 0$ and $\mu_q = 0$

In this subsection, we consider the case of  $\mu_l = \mu_q = 0$  and  $m_0 = 5.5$  MeV. The chiral condensate  $\sigma$  and the Polyakov loop  $\Phi$  are approximate order parameters of the chiral and deconfinement transitions, respectively. Figure 1(a) shows  $T$  dependence of  $\sigma$  and  $\Phi$  calculated with the PNJL model. Both the

chiral restoration and the deconfinement transition are seen to be crossover. The chiral restoration starts at the same temperature ( $T \approx 170$  MeV) as the deconfinement transition does, but the former transition is slower than the latter transition. Consequently, the pseudocritical temperature  $T_\sigma$  of the chiral restoration becomes higher than that  $T_\Phi$  of the deconfinement transition. Actually, it is found that  $T_\sigma = 216$  MeV and  $T_\Phi = 173$  MeV [52], when the pseudocritical temperatures are defined by the peak positions of  $\sigma$  and  $\Phi$ , respectively [45]. Figure 1(b) shows  $T$  dependence of  $\sigma$  and  $\Phi$  calculated with the EPNJL model. The chiral restoration occurs with the same speed as the deconfinement transition, so that  $T_\sigma = T_\Phi = 173$  MeV [63].

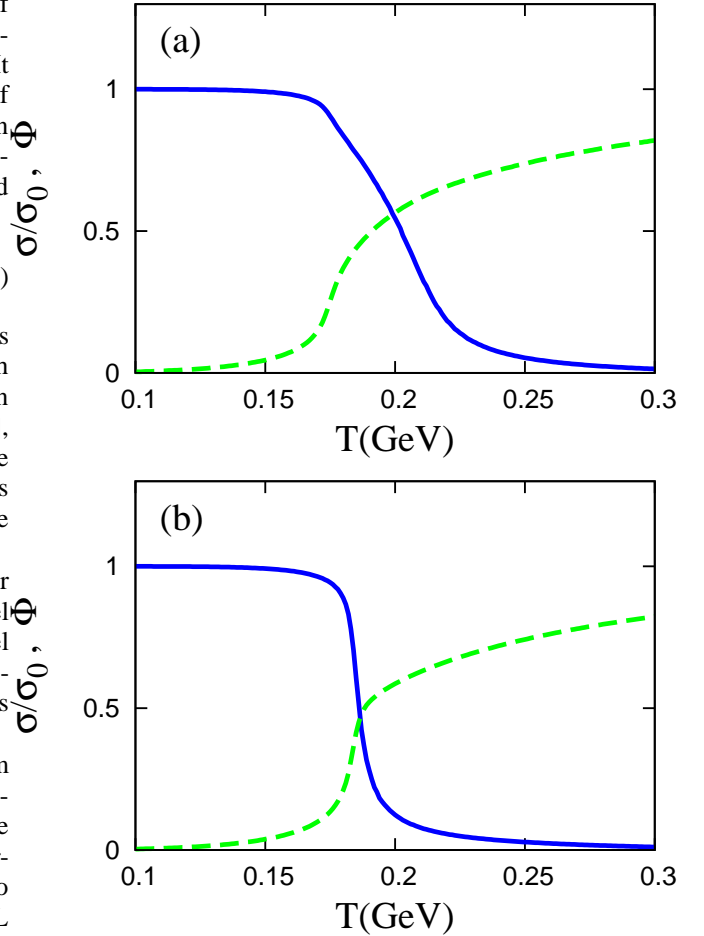


Fig. 1: (color online).  $T$  dependence of the chiral condensate  $\sigma$  and the Polyakov loop  $\Phi$  at  $\mu_l = 0$  and  $\mu_q = 0$  calculated with (a) the PNJL model and (b) the EPNJL model. The solid (dashed) line represents  $\sigma$  ( $\Phi$ ). Here,  $\sigma$  is normalized by the value  $\sigma_0$  at vacuum.

When two transitions are first order, they might coincide exactly [97]. At zero  $\mu_q$ , however, the chiral and deconfinement transitions are found to be crossover [85, 86]. There is hence no a priori reason why the two crossovers coincide exactly. In LQCD simulations at zero chemical potential [85, 98, 99], actually, there is a debate whether the transitions really coincide or not; see Ref. [80] and references therein.

The coincidence problem has conceptual difficulty, since  $\sigma$  and  $\Phi$  are approximate order parameters of the chiral and deconfinement transitions. This point can be circumvented by considering exact phase transitions relevant to the chiral and deconfinement crossovers. In the previous work [66], we found that the chiral and deconfinement transitions coincide when the  $P$  restoration and the  $C$  violation occur simultaneously at  $\theta = \Theta = \pi$ . The chiral restoration at  $\theta = \Theta = 0$  is a remnant of the  $P$  restoration at  $\theta = \Theta = \pi$ , whereas the deconfinement crossover at  $\theta = \Theta = 0$  is a remnant of the  $C$  violation at  $\theta = \Theta = \pi$ . Note that the  $P$  restoration and  $C$  violation are exact phase transitions. This theoretical prediction, however, cannot be confirmed by LQCD, since LQCD has the sign problem at finite  $\theta$ . The region of  $\mu_I > m_\pi/2$  and  $\Theta = \pi$  that we consider in this paper does not suffer from the sign problem.

### B. Results at finite $\mu_I$ and $\mu_q = 0$

When  $\mu_I > m_\pi/2$ , the pion condensation becomes finite at low temperature, so that  $P$  symmetry is spontaneously broken there [74]. In contrast, the pion condensate  $\pi$  is zero at  $\mu_I \leq m_\pi/2$ , so that  $P$  symmetry is preserved there. Figure 2 shows  $T$  dependence of the pion condensate at  $\mu_I = m_\pi$  and  $\mu_q = 0$ . The pion condensation disappears at  $T > T_P = 201(170)$  MeV in the PNJL (EPNJL) model.

Figure 3 shows the approximate order parameter  $\sqrt{\sigma^2 + \pi^2}$  of the chiral transition as a function of  $T$  and  $\mu_I$  calculated with the EPNJL model, where  $\Theta = 0$ . As for  $\mu_I > m_\pi/2$  where  $P$  symmetry is broken at small  $T$  and preserved at large  $T$ ,  $\sqrt{\sigma^2 + \pi^2}$  has either a cusp or a discontinuity, as expected. These singularities in  $\sqrt{\sigma^2 + \pi^2}$  come from the fact that the pion condensate  $\pi$  has either a cusp or a discontinuity there; more precisely, the  $P$  restoration is second order at  $m_\pi/2 < \mu_I < 95$  MeV and first order at  $\mu_I > 95$  MeV. As for  $\mu_I < m_\pi/2$  where the pion condensation vanishes and hence  $P$  symmetry is preserved, in contrast,  $\sqrt{\sigma^2 + \pi^2}$  changes smoothly. However, the change is still rapid, since  $\sigma$  has a rapid change. The rapid change of  $\sigma$  is nothing but the chiral restoration at zero and small  $\mu_I$ . Thus, the chiral restoration at zero  $\mu_I$  can be regarded as a remnant of the  $P$  restoration at  $\mu_I > m_\pi/2$ .

### C. Results at $\mu_I = 0$ and $\Theta = \pi$

When  $\Theta = \pi$ , the RW transition takes place at higher  $T$ . Hence  $C$  symmetry is spontaneously broken there [55, 66]. As an order parameter of the  $C$  violation, we can consider  $\Theta$ -odd quantities such as the quark number density  $n_q$  or the phase  $\psi$  of the modified Polyakov loop. Figure 4 shows  $T$  dependence of  $\sigma$ ,  $|\psi|$  and  $|n_q|$  at  $\mu_I = 0$  and  $\Theta = \pi$ . Note that  $n_q$  is pure imaginary and hence  $|n_q| = |\text{Im}(n_q)|$ . In the PNJL (EPNJL) model, the  $C$  violation occurs at  $T > T_C = 189(185)$  MeV, since  $n_q$  and  $\psi$  are finite there.

Figure 5 shows  $T$  and  $\Theta$  dependences of the approximate order parameter  $|\Phi|$  of the deconfinement transition calculated

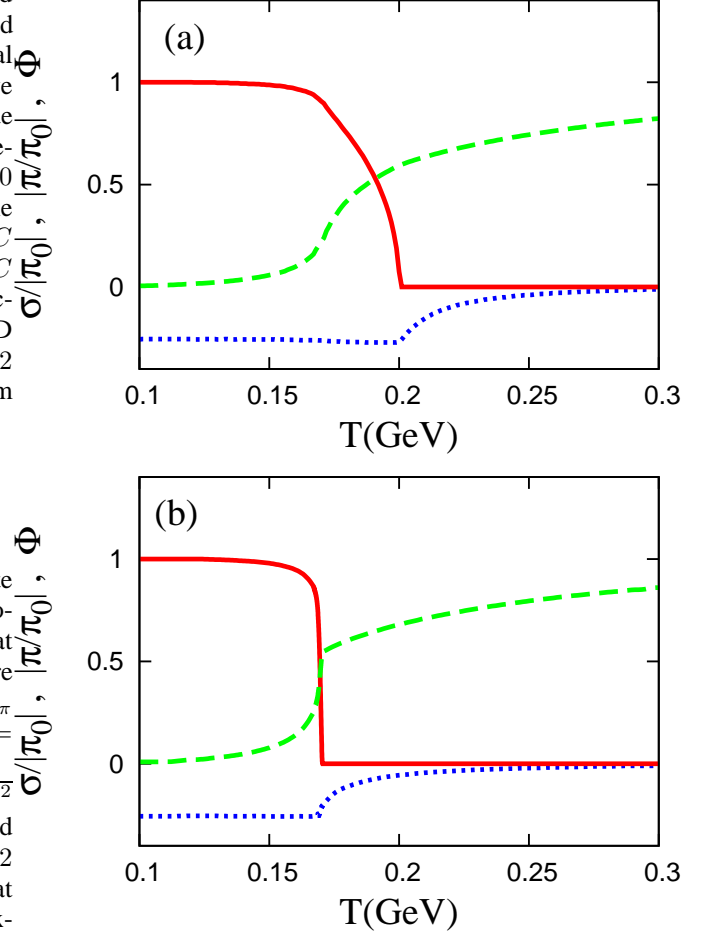


Fig. 2: (color online).  $T$  dependence of chiral condensate  $\sigma$ , pion condensation  $\pi$  and Polyakov loop  $\Phi$  at  $\mu_I = m_\pi$  and  $\mu_q = 0$  calculated with (a) the PNJL model and (b) the EPNJL model. The solid (dashed, dotted) line represents  $\pi$  ( $\Phi$ ,  $\sigma$ ). Here  $\sigma$  and  $\pi$  are normalized by  $|\pi_0|$ , where  $\pi_0 = \pi(T = 0)$ .

with the EPNJL model; here the case of  $\mu_I = 0$  is considered. Since  $|\Phi|$  is  $\Theta$ -even and has the RW periodicity, we can consider the region  $0 \leq \Theta \leq \pi/3$  only. There appears a first order phase transition at  $\Theta = \pi/3$ . This is the RW phase transition in which  $C$  symmetry is spontaneously broken. The transition becomes crossover as  $\Theta$  decreases from  $\pi/3$ . However, a smooth but rapid change remains even at  $\Theta = 0$ . The rapid change is nothing but the deconfinement transition at zero  $\mu_q$ . Thus, the deconfinement transition at zero  $\mu_q$  is a remnant of the first-order RW phase transition at  $\Theta = \pi/3$  [55, 66].

### D. Results at finite $\mu_I$ and $\Theta$

Figure 6 shows  $T$  dependence of the pion condensate  $\pi$  and the phase  $\psi$  of  $\Psi$  at  $\mu_I = m_\pi$  and  $\Theta = \pi$ . In the PNJL (EPNJL) model,  $P$  symmetry is spontaneously broken below  $T_P = 250(196)$  MeV as shown by a finite value of the pion

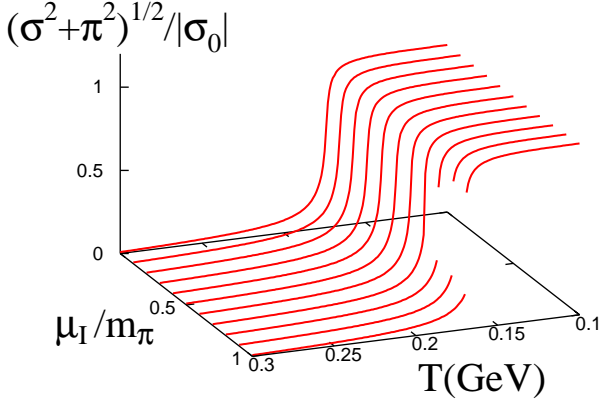


Fig. 3: (color online). The order parameter  $\sqrt{\sigma^2 + \pi^2}$  of the chiral transition as a function of  $T$  and  $\mu_I$  plane calculated with the EPNJL model. Here we consider the case of  $\mu_q = 0$ .

condensate. In contrast,  $\tilde{C}$  symmetry is spontaneously violated above  $T_{\tilde{C}} = 188(184)\text{MeV}$  as indicated by a finite value of  $\psi$ . Thus  $P$  and/or  $\tilde{C}$  symmetries are always broken at any temperature. This situation is the same as that at  $\theta = \Theta = \pi$  [66]. The difference  $\Delta T \equiv T_P - T_{\tilde{C}}$  is smaller in the EPNJL model than in the PNJL model. The entanglement interaction thus makes  $\Delta T$  very small, although the two transitions do not coincide exactly. Note that at  $\mu_I = m_\pi$  the  $P$  restoration is second order whereas the  $\tilde{C}$  violation is first order in both the PNJL and EPNJL models. Comparing Fig. 6 with Fig. 2, one can see that  $T_P$  goes up as  $\Theta$  increases.

Figure 7 shows the same quantities as Fig. 6, except the case of  $\mu_I = 600\text{MeV}$  is considered. In both the PNJL and EPNJL models, the  $P$  restoration and the  $\tilde{C}$  violation occur at the same temperature, more precisely  $T_P = T_{\tilde{C}} = 160\text{ MeV}$  for the PNJL model and  $147\text{ MeV}$  for the EPNJL model. This is because the  $P$  restoration becomes sharper and eventually first-order as  $\mu_I$  increases. Thus the first-order nature of the  $P$  restoration makes the  $\tilde{C}$  violation strong first-order and consequently attracts the  $\tilde{C}$  violation.

Figure 8 shows the phase diagram in the  $\mu_I$ - $T$  plane at  $\Theta = \pi$ . The  $P$  violation due to the pion condensation occur at  $\mu_I > m_\pi/2$  and lower  $T$ . The  $P$  restoration with respect to increasing  $T$  is second-order at  $\mu_I < 480(450)\text{ MeV}$  and first-order at  $\mu_I > 480(450)\text{ MeV}$  in the PNJL (EPNJL) model. The  $\tilde{C}$  violation is always first order. When  $\mu_I > 600(545)\text{ MeV}$ , the  $P$  restoration coincides with the  $\tilde{C}$  violation in the PNJL (EPNJL) model, as already mentioned in Fig. 7. The region where  $P$  and  $\tilde{C}$  symmetries are violated simultaneously is tiny in the EPNJL model compared with the case of the PNJL model.

Figure 9 shows  $\Theta$  dependence of the pion condensation  $\pi$  and the imaginary part of the quark number density  $n_q$  calculated with the PNJL model; note that  $n_q$  is pure imaginary in this case. In panel (a) where  $T = 180\text{ [MeV]} < T_C = 188\text{ [MeV]}$ , both  $\pi$  and  $n_q$  are smooth functions of  $\Theta$  and

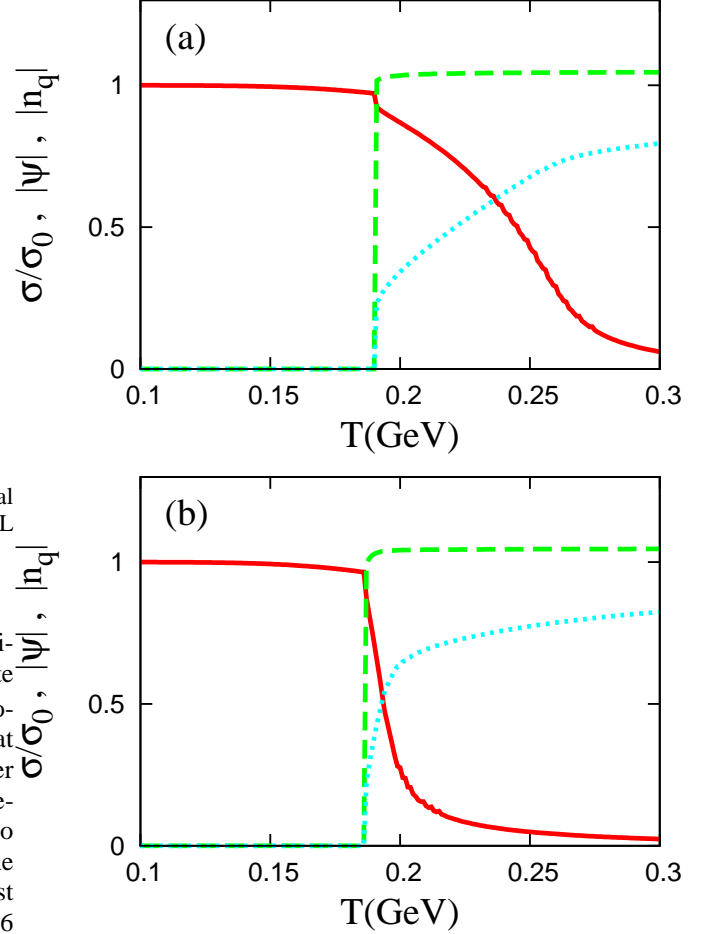


Fig. 4: (color online).  $T$  dependence of  $\sigma$ ,  $|\psi|$  and  $|n_q|$  at  $\mu_I = 0$  and  $\Theta = \pi$  calculated with (a) the PNJL model and (b) the EPNJL model. The solid (dashed, dotted) line represents  $\sigma$  ( $|\psi|$ ,  $|n_q|$ ). Here,  $\sigma$  is normalized by the value  $\sigma_0$  at vacuum and  $n_q$  is by  $N_f T^3$ , where  $N_f = 2$ .

no RW phase transition is seen at  $\Theta = \pi/3 \bmod 2\pi/3$ . In panel (b) where  $T = 220\text{ [MeV]} > T_C$ , the  $\Theta$ -even quantity  $\pi$  has a cusp at  $\Theta = \pi/3 \bmod 2\pi/3$ , whereas the  $\Theta$ -odd quantity  $n_q$  is discontinuous there [54]. This singularity is called the RW phase transition. The pion condensate is finite only around  $\Theta = \pi/3 \bmod 2\pi/3$  and vanishes when  $T_P < 220\text{ MeV}$ . This behavior of  $\pi$  resembles that of  $\sigma$  in the case of  $m_0 = \mu_I = 0$  [47] where  $\sigma$  and  $\pi$  are completely symmetric.

Figure 10 shows the phase diagram in the  $\Theta$ - $T$  plane at  $\mu_I = m_\pi$  calculated with (a) the PNJL model and (b) the EPNJL model. The phase diagram is  $\Theta$ -even and has the RW periodicity. The RW transition at  $\Theta = \pi/3 \bmod 2\pi/3$  is first order. The deconfinement transition is first-order in the vicinity of the endpoint of the RW transition, crossover for other  $\Theta$ . The  $P$  restoration is always second order in the PNJL model. In the EPNJL model, the  $P$  restoration is first-order at  $\Theta/(\pi/3) = -0.3 \sim 0.3, 1.7 \sim 2.3, 3.7 \sim 4.3$  and second



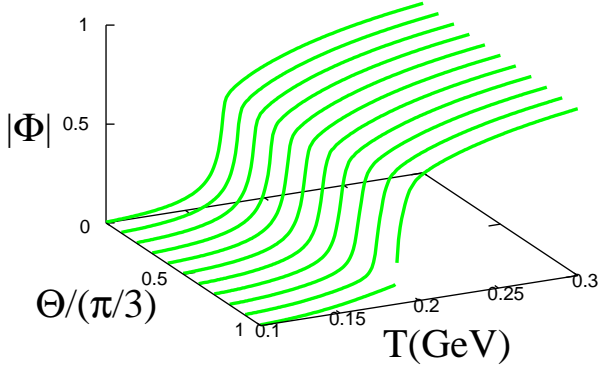


Fig. 5: (color online). The approximate order parameter  $|\Phi|$  of the deconfinement transition as a function of  $T$  and  $\theta$  calculated with the EPNJL model. Here the case of  $\mu_I = 0$  is taken.

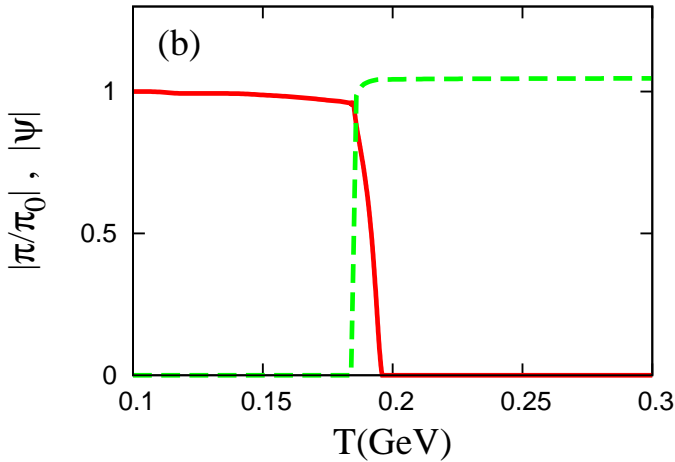
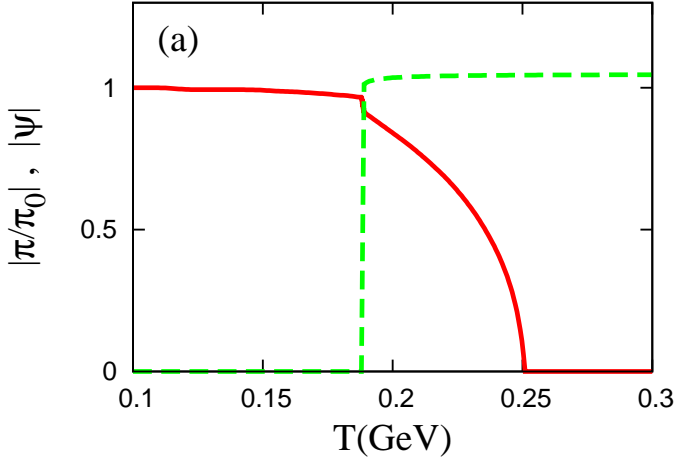


Fig. 6: (color online).  $T$  dependence of the pion condensate  $\pi$  and the phase  $\psi$  of  $\Psi$  at  $\mu_I = m_\pi$  and  $\Theta = \pi$  calculated with (a) the PNJL model and (b) the EPNJL model. The solid (dashed) line represents  $|\pi|$  ( $|\psi|$ ) and  $\pi$  is normalized by the value  $\pi_0$  at  $T = 0$ .

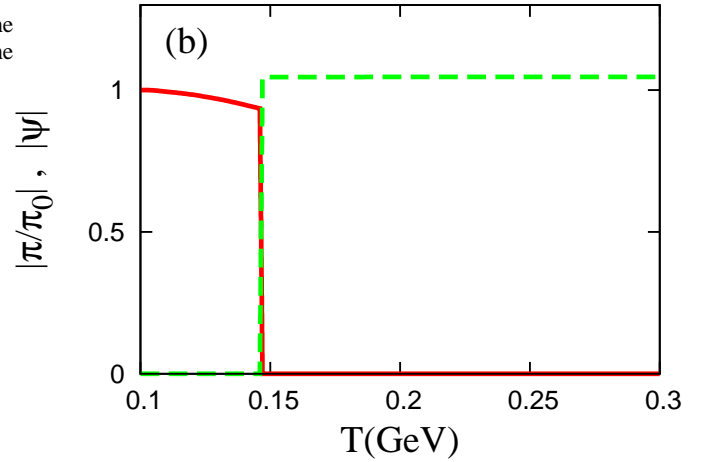
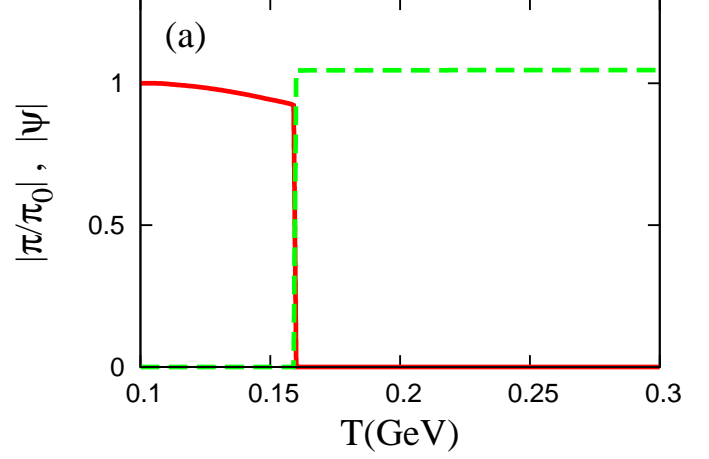


Fig. 7: (color online).  $T$  dependence of the pion condensate  $\pi$  and the phase  $\psi$  of  $\Psi$  at  $\mu_I = 600$  MeV and  $\Theta = \pi$  calculated with (a) the PNJL model and (b) the EPNJL model. See Fig. 6 for the definition of lines.

order for other  $\Theta$ . Thus the imaginary quark chemical potential makes the  $P$  restoration weaker. In the regions where the  $P$  restoration is first-order, the  $P$  restoration and the deconfinement transition almost coincide with each other in the EPNJL model.

#### IV. SUMMARY

We have studied the interplay between the pion-superfluidity and RW phase transitions at real isospin and imaginary quark chemical potential, using the PNJL and EPNJL models. In the region of  $\Theta = \pi$  and  $\mu_I > m_\pi/2$ , parity symmetry ( $P$ ) and charge-conjugation symmetry ( $\tilde{C}$ ) are spontaneously broken by the pion-superfluidity and RW transitions, respectively. The chiral and deconfinement crossovers at zero isospin and quark chemical potentials are remnants of these exact phase transitions, i.e. the  $P$  restoration and the  $\tilde{C}$  violation, respectively. The chiral and deconfine-



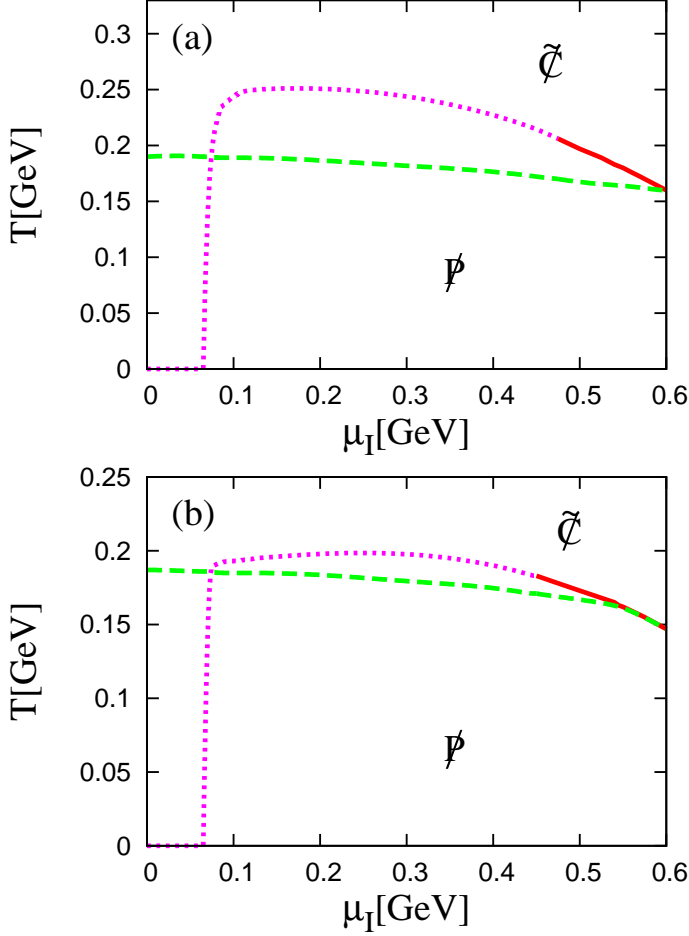


Fig. 8: (color online). Phase diagram in the  $\mu_I$ - $T$  plane at  $\Theta = \pi$  calculated with (a) the PNJL model and (b) the EPNJL model. The dashed (solid) line represents the second (first) order  $P$  transition, while the dotted line represents the first order  $\tilde{C}$  transition.

ment crossovers almost coincide when  $\Delta T = T_P - T_{\tilde{C}}$  is small. The interplay between the chiral and deconfinement crossovers at zero isospin and quark chemical potential is thus determined by the correlation between the  $P$  restoration and the  $\tilde{C}$  violation at  $\mu_I > m_\pi/2$  and  $\Theta = \pi$ .

At  $\mu_I \gtrsim 4m_\pi$ , the  $P$  restoration becomes first-order and hence the  $P$  restoration and the  $\tilde{C}$  violation take place simultaneously. The  $P$  restoration and the  $\tilde{C}$  violation are strongly correlated with each other in this region. The correlation is weakened as  $\mu_I$  decreases from  $4m_\pi$ . At  $\mu_I \approx m_\pi \sim 2m_\pi$ , the critical temperature of the  $P$  restoration is larger than that of the  $\tilde{C}$  violation by 10 MeV in the case of the EPNJL model and by 60 MeV in the case of the PNJL model. As a consequence of this property, at zero isospin and quark chemical potentials, the pseudocritical temperature of the chiral transition is larger than that of the deconfinement transition by only a few MeV in the case of the EPNJL model and by 50 MeV in the case of the PNJL model. The correlation between the  $P$  restoration and the  $\tilde{C}$  violation at  $\mu_I \approx m_\pi \sim 2m_\pi$  and

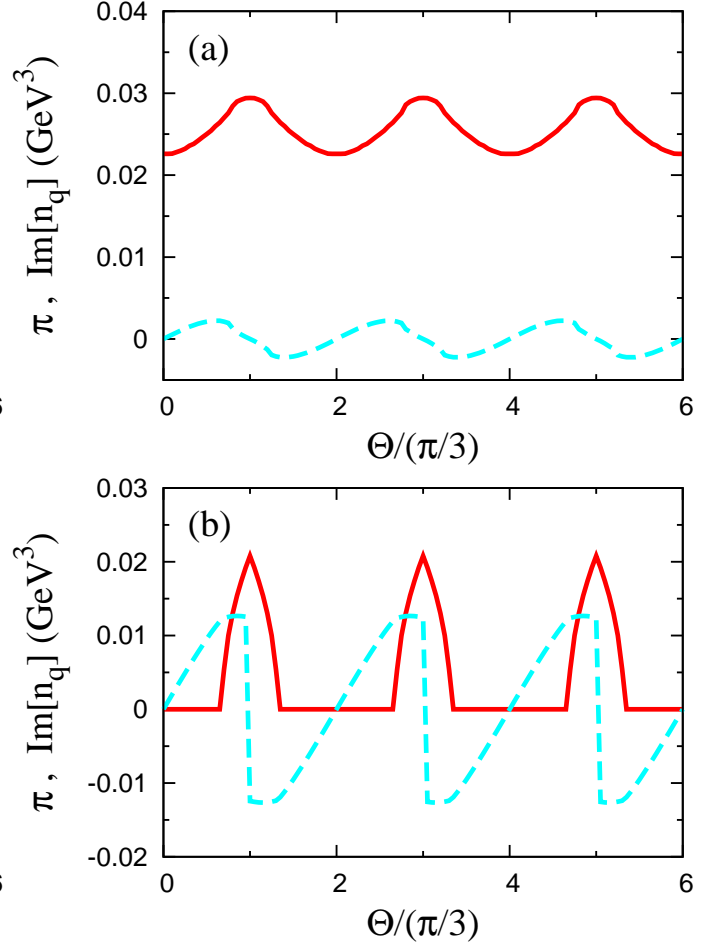


Fig. 9: (color online).  $\Theta$  dependence of the pion condensate  $\pi$  and the imaginary part  $\text{Im}(n_q)$  of quark number density calculated with the PNJL model. Here the case of  $\mu_I = m_\pi$  is taken. Quantities are shown in  $\text{GeV}^3$ . Panel (a) is for the case of  $T = 180$  MeV and panel (b) is for the case of  $T = 220$  MeV. The solid (dotted) line represents  $\pi$  ( $\text{Im}(n_q)$ ).

$\Theta = \pi$  is thus the key to determining the interplay between the chiral restoration and the deconfinement transition at zero isospin and quark chemical potentials.

The theoretical prediction at  $\Theta = \pi$  and finite  $\mu_I$  can be checked by LQCD, since LQCD has no sign problem there. Furthermore, the  $P$  restoration and the  $\tilde{C}$  violation are exact phase transitions and hence we can define the order parameters exactly. In future, we can thus determine the critical temperatures of the exact phase transitions without any ambiguity by using LQCD. LQCD analyses along this line may give an insight into the coincidence problem between the chiral restoration and the deconfinement transition at zero isospin and quark number chemical potentials. Furthermore, we may get knowledge of the phase diagram and the equation of state at real  $\mu_I$  and real  $\mu_q$  by the extrapolation from real  $\mu_I$  and imaginary  $\mu_q$ .

It may be also interesting to study the QCD phase diagram in the region where all of  $\Theta$ ,  $\mu_I$ ,  $\theta$  and  $T$  are finite. For

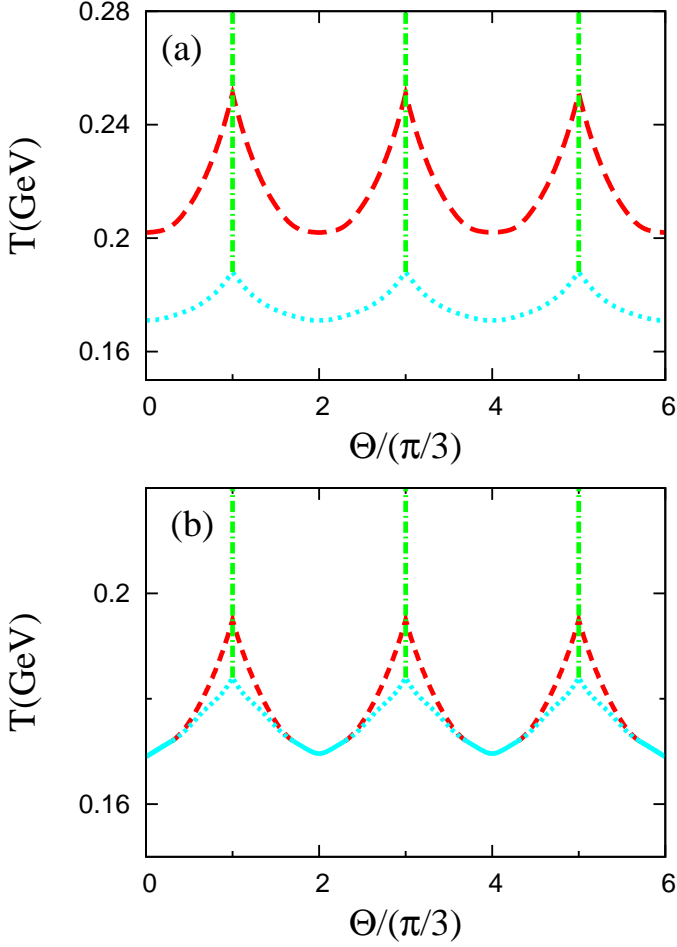


Fig. 10: (color online). Phase diagram in the  $\theta$ - $T$  plane at  $\mu_I = m_\pi$  calculated with (a) the PNJL model and (b) the EPNJL model. The dot-dashed lines stand for the RW transition, and the dotted lines represent the deconfinement transition. The solid (dashed) lines denote the  $P$  restoration of first-order (second-order).

$\Theta = \mu_I = \theta = 0$  and small or zero  $T$ , only  $\sigma$  is finite. For large  $\mu_I$  and low  $T$ ,  $\pi$  is the largest condensate instead of  $\sigma$ . At large  $\theta$  and low  $T$ , meanwhile,  $\eta$  is the largest one. For large values of  $\mu_I$  and  $\theta$ , it was shown by the NJL model [26] that, instead of  $\pi$  or  $\eta$ , the charged-scalar and isovector condensate  $a_0^\pm$  can condense at low  $T$ . In this case, the  $U_{I_3}(1)$  symmetry under the transformation induced by the isospin generator  $\tau_3$  is spontaneously broken, whereas parity symmetry is not broken. In principle, one can discuss the coincidence between the  $U_{I_3}(1)$  breaking and the RW transition by using the PNJL model. The calculation, however, is quite time-consuming. This analysis is then an interesting future work.

#### Acknowledgments

Authors thank A. Nakamura, T. Inagaki, M. Matsuzaki, T. Saito, S. Nakamura, K. Morita, K. Nagata and K. Kashiwa for useful discussions and comments. M.K. and H. K. also thank M. Imachi, H. Yoneyama, H. Aoki, M. Tachibana and K. Fukuda for useful discussions and comments. T.S. and Y. S. are supported by JSPS. This calculation was partially carried out on SX-8 at Research Center for Nuclear Physics, Osaka University.

- 
- [1] J. B. Kogut and D. K. Sinclair Phys. Rev. D **77**, 114503 (2008).
  - [2] Z. Fodor, and S. D. Katz, Phys. Lett. B **534**, 87 (2002); J. High Energy Phys. **03**, 014 (2002).
  - [3] C. R. Allton, S. Ejiri, S. J. Hands, O. Kaczmarek, F. Karsch, E. Laermann, Ch. Schmidt, and L. Scorzato, Phys. Rev. D **66**, 074507 (2002); C. R. Allton, S. Ejiri, S. J. Hands, O. Kaczmarek, F. Karsch, E. Laermann, and C. Schmidt, Phys. Rev. D **68**, 014507 (2003); S. Ejiri, C. R. Allton, S. J. Hands, O. Kaczmarek, F. Karsch, E. Laermann, and C. Schmidt, Prog. Theor. Phys. Suppl. **153**, 118 (2004).
  - [4] P. de Forcrand and O. Philipsen, Nucl. Phys. **B642**, 290 (2002); P. de Forcrand and O. Philipsen, Nucl. Phys. **B673**, 170 (2003).
  - [5] M. D'Elia and M. P. Lombardo, Phys. Rev. D **67**, 014505 (2003); Phys. Rev. D **70**, 074509 (2004); M. D'Elia, F. D. Renzo, and M. P. Lombardo, Phys. Rev. D **76**, 114509 (2007);
  - [6] H. S. Chen and X. Q. Luo, Phys. Rev. **D72**, 034504 (2005); arXiv:hep-lat/0702025 (2007); L. K. Wu, X. Q. Luo, and H. S. Chen, Phys. Rev. **D76**, 034505 (2007).
  - [7] M. D'Elia and F. Sanfilippo, Phys. Rev. D **80**, 014502 (2009).
  - [8] P. Cea, L. Cosmai, M. D'Elia, C. Manneschi and A. Papa, Phys. Rev. D **80**, 034501 (2009).
  - [9] M. D'Elia and F. Sanfilippo, Phys. Rev. D **80**, 111501 (2009).
  - [10] P. de Forcrand and O. Philipsen, Phys. Rev. Lett. **105**, 152001 (2010).
  - [11] K. Nagata, A. Nakamura, Y. Nakagawa, S. Motoki, T. Saito and M. Hamada, Proc. Sci. LAT2009 (2009) 191 [arXiv:0911.4164](2009); K. Nagata, and A. Nakamura, arXiv:1104.2142 [hep-ph] (2011).
  - [12] T. Takaishi, P. de Forcrand and A. Nakamura, Proc. Sci. LAT2009 (2009) 198 [arXiv:1002.0890](2010).
  - [13] Y. Nambu and G. Jona-Lasinio, Phys. Rev. **122**, 345 (1961); Phys. Rev. **124**, 246 (1961).
  - [14] M. Asakawa and K. Yazaki, Nucl. Phys. **A504**, 668 (1989).
  - [15] S. Klimt, M. Lutz, U. Vogl, and W. Weise, Nucl. Phys. **A516**, 429 (1990).

- [16] U. Vogl, M. Lutz, S. Klimt, and W. Weise, Nucl. Phys. **A516**, 469 (1990).
- [17] S. P. Klevansky Rev. Mod. Phys. **64**, 649 (1992).
- [18] T. Hatsuda and T. Kunihiro Phys. Rep. **247**, 221 (1994).
- [19] H. Fujii, Phys. Rev. D **67**, 094018 (2003).
- [20] M. Buballa Phys. Rep. **407**, 205 (2005).
- [21] A. Barducci, R. Casalbuoni, G. Pettini, and L. Ravagli, Phys. Rev. D **72**, 056002 (2005).
- [22] L. He, M. Jin, and P. Zhuang, Phys. Rev. D **71**, 116001 (2005).
- [23] A. A. Osipov, B. Hiller, and J. da Providência, Phys. Lett. B **634**, 48 (2006); A. A. Osipov, B. Hiller, J. Moreira, and A. H. Blin, Eur. Phys. J. C **46**, 225 (2006).
- [24] K. Kashiwa, H. Kouno, T. Sakaguchi, M. Matsuzaki, and M. Yahiro, Phys. Lett. B **647**, 446 (2007); K. Kashiwa, M. Matsuzaki, H. Kouno, and M. Yahiro, Phys. Lett. B **657**, 143 (2007).
- [25] T. Fujihara, T. Inagaki, and D. Kimura, Prog. Theor. Phys. **117**, 139 (2007).
- [26] D. Boer and J. K. Boomsma, Phys. Rev. D **78**, 054027 (2008).
- [27] J. K. Boomsma and D. Boer, Phys. Rev. D **80**, 034019 (2009).
- [28] A. J. Mizher, and E. S. Fraga, Nucl. Phys. A **820**, 247c (2009); Nucl. Phys. A **831**, 91 (2009);
- [29] P. N. Meisinger, and M. C. Ogilvie, Phys. Lett. B **379**, 163 (1996).
- [30] A. Dumitru, and R. D. Pisarski, Phys. Rev. D **66**, 096003 (2002); A. Dumitru, Y. Hatta, J. Lenaghan, K. Orginos, and R. D. Pisarski, Phys. Rev. D **70**, 034511 (2004); A. Dumitru, R. D. Pisarski, and D. Zschesche, Phys. Rev. D **72**, 065008 (2005).
- [31] K. Fukushima, Phys. Lett. B **591**, 277 (2004).
- [32] S. K. Ghosh, T. K. Mukherjee, M. G. Mustafa, and R. Ray, Phys. Rev. D **73**, 114007 (2006).
- [33] E. Megías, E. R. Arriola, and L. L. Salcedo, Phys. Rev. D **74**, 065005 (2006).
- [34] C. Ratti, M. A. Thaler, and W. Weise, Phys. Rev. D **73**, 014019 (2006); C. Ratti, S. Rößner, M. A. Thaler, and W. Weise, Eur. Phys. J. C **49**, 213 (2007).
- [35] S. Rößner, C. Ratti, and W. Weise, Phys. Rev. D **75**, 034007 (2007).
- [36] Z. Zhang, and Y. -X. Liu, Phys. Rev. C **75**, 064910 (2007).
- [37] S. Mukherjee, M. G. Mustafa, and R. Ray, Phys. Rev. D **75**, 094015 (2007).
- [38] M. Ciminale, R. Gatto, N. D. Ippolito, G. Nardulli, and M. Ruggieri, Phys. Rev. D **77**, 054023 (2008); M. Ciminale, R. Gatto, G. Nardulli, and M. Ruggieri, Phys. Lett. B **657**, 64 (2007).
- [39] H. Hansen, W. M. Alberico, A. Beraudo, A. Molinari, M. Nardi, and C. Ratti, Phys. Rev. D **75**, 065004 (2007).
- [40] C. Sasaki, B. Friman, and K. Redlich, Phys. Rev. D **75**, 074013 (2007).
- [41] B. -J. Schaefer, J. M. Pawłowski, and J. Wambach, Phys. Rev. D **76**, 074023 (2007).
- [42] R. Rößner, T. Hell, C. Ratti, and W. Weise, Nucl. Phys. A **814**, 118 (2008).
- [43] T. Hell, R. Rößner, M. Cristoforetti, and W. Weise, Phys. Rev. D **79**, 014022 (2009).
- [44] P. Costa, C. A. de Sousa, M. C. Ruivo, and H. Hansen, Europhys. Lett. **86**, 31001 (2009). P. Costa, M. C. Ruivo, C. A. de Sousa, H. Hansen, and W. M. Alberico, Phys. Rev. D **79**, 116003 (2009).
- [45] K. Kashiwa, H. Kouno, M. Matsuzaki, and M. Yahiro, Phys. Lett. B **662**, 26 (2008); K. Kashiwa, M. Matsuzaki, H. Kouno, Y. Sakai, and M. Yahiro, Phys. Rev. D **79**, 076008 (2009); K. Kashiwa, H. Kouno, and M. Yahiro, Phys. Rev. D **80**, 117901 (2009).
- [46] K. Fukushima, Phys. Rev. D **77**, 114028 (2008).
- [47] Y. Sakai, K. Kashiwa, H. Kouno, and M. Yahiro, Phys. Rev. D **77**, 051901 (2008).
- [48] Y. Sakai, K. Kashiwa, H. Kouno, and M. Yahiro, Phys. Rev. D **78**, 036001 (2008); Y. Sakai, K. Kashiwa, H. Kouno, M. Matsuzaki, and M. Yahiro, Phys. Rev. D **78**, 076007 (2008); Y. Sakai, T. Sasaki, H. Kouno, and M. Yahiro, Phys. Rev. D **82**, 096007 (2010).
- [49] W. J. Fu, Z. Zhang, and Y. X. Liu, Phys. Rev. D **77**, 014006 (2008).
- [50] H. Abuki, M. Ciminale, R. Gatto, G. Nardulli, and M. Ruggieri, Phys. Rev. D **77**, 074018 (2008); H. Abuki, M. Ciminale, R. Gatto, N. D. Ippolito, G. Nardulli, and M. Ruggieri, Phys. Rev. D **78**, 014002 (2008).
- [51] H. Abuki, R. Anglani, R. Gatto, G. Nardulli, and M. Ruggieri, Phys. Rev. D **78**, 034034 (2008).
- [52] Y. Sakai, K. Kashiwa, H. Kouno, M. Matsuzaki, and M. Yahiro, Phys. Rev. D **79**, 096001 (2009).
- [53] L. McLerran K. Redlich and C. Sasaki, Nucl. Phys. A **824**, 86 (2009).
- [54] K. Kashiwa, M. Yahiro, H. Kouno, M. Matsuzaki, and Y. Sakai, J. Phys. G: Nucl. Part. Phys. **36**, 105001 (2009).
- [55] H. Kouno, Y. Sakai, K. Kashiwa, and M. Yahiro, J. Phys. G: Nucl. Part. Phys. **36**, 115010 (2009).
- [56] T. Hell, S. Rößner, M. Cristoforetti, and W. Weise, Phys. Rev. D **81**, 074034 (2010); T. Hell, K. Kashiwa, and W. Weise, Phys. Rev. D **83**, 114008 (2011).
- [57] Y. Sakai, H. Kouno, and M. Yahiro, J. Phys. G: Nucl. Part. Phys. **37**, 105007 (2010).
- [58] A. Bhattacharyya, P. Deb, S. K Ghosh, and R. Ray, Phys. Rev. D **82**, 014021 (2010).
- [59] K. Fukushima, M. Ruggieri, and R. Gatto, Phys. Rev. D **81**, 114031 (2010).
- [60] T. Matsumoto, K. Kashiwa, H. Kouno, K. Oda, and M. Yahiro, Phys. Lett. B **694**, 367 (2011).
- [61] C. A. Contrera, M. Orsaria, and N. N. Scoccola, Phys. Rev. D **82**, 054026 (2010).
- [62] T. Sasaki, Y. Sakai, H. Kouno and M. Yahiro, Phys. Rev. D **82**, 116004 (2010).
- [63] Y. Sakai, T. Sasaki, H. Kouno and M. Yahiro, Phys. Rev. D **82**, 076003 (2010).
- [64] R. Gatto, and M. Ruggieri, Phys. Rev. D **82**, 054027 (2010).
- [65] R. Gatto, and M. Ruggieri, Phys. Rev. D **83**, 034016 (2011).
- [66] H. Kouno, Y. Sakai, T. Sasaki, K. Kashiwa, and M. Yahiro, Phys. Rev. D **83**, 076009 (2011).
- [67] Y. Sakai, T. Sasaki, H. Kouno and M. Yahiro, arXiv:1104.2394 [hep-ph].
- [68] Y. Sakai, H. Kouno, T. Sasaki and M. Yahiro, , arXiv:1105.0413 [hep-ph]; T. Sasaki, Y. Sakai, H. Kouno and M. Yahiro, , arXiv:1105.3959 [hep-ph].
- [69] K. Kashiwa, Phys. Rev. D **83**, 117901 (2011).
- [70] V. Pagura, D. Gomez Dumm, and N. N. Scoccola, arXiv:1105.1739 [hep-ph](2011).
- [71] K. Kashiwa, T. Hell, and W. Weise, Phys. Rev. D **84**, 056010 (2011).
- [72] K. Morita, V. Skokov, B. Friman, and K. Redlich, arXiv:1107.2273 [hep-ph](2011); arXiv:1108.0735 [hep-ph](2011).
- [73] A. Roberge and N. Weiss, Nucl. Phys. **B275**, 734 (1986).
- [74] D. T. Son and M. A. Stephanov, Phys. Rev. Lett. **86**, 592 (2001).
- [75] J. B. Kogut and D. K. Sinclair, Phys. Rev. D **70**, 094501 (2004).
- [76] Y. Nishida, Phys. Rev. D **69**, 094501 (2004).

- [77] L.F. Palhares, E.S. Fraga, and C. Villavicencio, Nucl. Phys. **A820**, 287c (2009); E.S. Fraga, L. F. Palhares, and C. Villavicencio, Phys. Rev. D **79**, 014021 (2009).
- [78] A. Barducci, R. Casalbuoni, S. DE Curtis, R. Gatto, and G. Pettini, Phys. Lett. B **231**, 463 (1989); A. Barducci, R. Casalbuoni, G. Pettini, and R. Gatto, Phys. Rev. D **49**, 426 (1994);
- [79] K. Nagata and A. Nakamura, private communications.
- [80] S. Borsányi, Z. Fodor, C. Hoelbling, S. D. Katz, S. Krieg, C. Ratti, and K. K. Szabo, arXiv:1005.3508 [hep-lat] (2010).
- [81] J. Cleymans, K. Redlich, H. Satz, and E. Suhonen, Z. Phys. C-Particle and Fields **33**,151 (1986).
- [82] H. Kouno, and F. Takagi, Z. Phys. C-Particle and Fields **42**, 209 (1989).
- [83] L. McLerran, and R. D. Pisarski, Nucl. Phys. **A796**, 83 (2007).
- [84] Y. Hidaka, L. McLerran, and R. D. Pisarski, Nucl. Phys. **A808**, 117 (2008).
- [85] F. Karsch, and E. Laermann, Phys. Rev. D **50**, 6954 (1994); F. Karsch, Lattice QCD at high temperature and density, [hep-lat/0106019], Lect. Notes Phys. **583**, 209-249 (2002).
- [86] Y. Aoki, G. Endrödi, Z. Fodor, S. D. Katz and K. K. Szabó, Nature **443**, 675 (2006).
- [87] G. Boyd, J. Engels, F. Karsch, E. Laermann, C. Legeland, M. Lütgemeier, and B. Petersson, Nucl. Phys. **B469**, 419 (1996).
- [88] O. Kaczmarek, F. Karsch, P. Petreczky, and F. Zantow, Phys. Lett. B **543**, 41 (2002).
- [89] F. Karsch, E. Laermann, and A. Peikert, Nucl. Phys. B **605**, 579 (2001).
- [90] O. Kaczmarek and F. Zantow, Phys. Rev. D **71**, 114510 (2005).
- [91] G. Aarts, S. P. Kumar and J. Rafferty, JHEP **07**, 056 (2010); J. Rafferty, arXiv:1103.2315 [hep-th](2011).
- [92] K.-I. Kondo, Phys. Rev. D **82**, 065024 (2010).
- [93] J. Braun, L. M. Haas, F. Marhauser, and J. M. Pawłowski, Phys. Rev. Lett. **106**, 022002 (2011); J. Braun, and A. Janot, arXiv:1102.4841[hep-ph] (2011).
- [94] T. K. Herbst, J. M. Pawłowski, and B. -J. Schaefer, Phys. Lett. B **696**, 58 (2011).
- [95] C. Wetterich, Phys. Lett. B **301**, 90 (1991).
- [96] M. D’Elia, S. Mukherjee and F. Sanfilippo, Phys. Rev. D **82**, 051501 (2010).
- [97] A. Barducci, R. Casalbuoni, G. Pettini, and R. Gatto, Phys. Lett. B **301**, 95 (1993).
- [98] S. Aoki, M. Fukugita, S. Hashimoto, N. Ishizuka, Y. Iwasaki, K. Kanaya, Y. Kuramashi, H. Mino, M. Okawa, A. Ukawa, and T. Yoshie, Phys. Rev. D **57**, 3910 (1998).
- [99] Y. Aoki, Z. Fodor, S. D. Katz, and K. K. Szabo, Phys. Lett. B **643**, 46 (2006); Y. Aoki, S. Borsanyi, S. Durr, Z. Fodor, S. D. Katz, S. Krieg, and K. K. Szabo, J. High Energy Phys. **0906**, 088 (2009).